Controllability analysis of the magnetic flux in ITER hybrid scenarios

S.Djordjevic[1], M. de Baar[1,2], M.Steinbuch[1], J.Citrin[2], G.M.D.Hogeweij[2]

[1] *Control Systems Technology, University of Eindhoven, Eindhoven, The Netherlands*

[2] *FOM-Institute for Plasma Physics Rijnhuizen, Association EURATOM-FOM, Trilateral Euregio Cluster, Nieuwegein, The Netherlands*

Introduction

One of the challenges for ITER is the development of model-based controllers for optimal plasma performance. Particular emphasis has to be given to the possible actuation strategies for the candidate plasma scenarios. One of the candidate plasma scenarios is the hybrid mode, in which the T_i profile is expected to be determined by the critical gradient for the onset of turbulent ion temperature gradient (ITG) driven transport. This critical gradient is explicitly dependent on the safety factor q and the magnetic shear s as $(\nabla T_i/T_i)_{\text{crit}} \sim (T_i/T_e)\cdot(1+s/q)$. These can be expressed as a function of the poloidal magnetic flux $\psi(t,x)$ in the radial coordinate x. For this reason, developing a model-based closed loop control strategy for the distribution of the poloidal magnetic flux $\psi(t,x)$ is expected to increase the fusion performance. As the hybrid scenario is MHD stable (no sawteeth, and hence no NTM drive) a suitable and available distributed actuator for $\psi(t,x)$ in the hybrid scenarios would be electron cyclotron current drive (ECCD).

In this contribution, we present a controllability analysis of $\psi(t,x)$ using a control-oriented model to identify the practically reachable $\psi(t,x)$ profiles for different j_{eccd} deposition. In Section 2, the control-oriented model introduced in [2] is reformulated in a state-space representation suitable for shaping the $\psi(t,x)$ profiles using spatially distributed controllers. The distribution of the ECCD current is chosen to be the system input, and the derived $\psi(t,x)$ profiles are the system outputs. Also in Section 2, we introduce the concept of controllability and observability, and the associated formalisms. In Section 3, we present the results, which are discussed and concluded in Section 4.

Control-oriented model of the magnetic flux

The poloidal magnetic flux $\psi(t,x)$ at any point in the poloidal cross section is the total flux through the surface S bounded by the toroidal ring passing through the point. Using cylindrical approximation for the domain $r\in[0,a]$, with $x\equiv r/a$ and neglecting the diamagnetic effect, the following flux profile evolution can be derived as suggested in [2]

$$\frac{\partial\psi(t,x)}{\partial t}=\frac{\eta_{\parallel}(x)}{\mu_0 a_{\text{e}}^2}\left(\frac{\partial^2\psi(t,x)}{\partial x^2}+\frac{1}{x}\frac{\partial\psi(t,x)}{\partial x}\right)+\eta_{\parallel}(x)R_0 j_{\text{ni}}(x), \tag{1}$$

where the non-inductive current density $j_{\mathrm{ni}}(x) = j_{\mathrm{bc}}(x) + j_{\mathrm{nbi}}(x) + j_{\mathrm{eccd}}(x)$. The boundary conditions at the plasma centre surface equals $\frac{\partial \psi(t,0)}{\partial x} = 0$ and at the last closed magnetic (LCMS) equals $\frac{\partial \psi(t,1)}{\partial x} = -\frac{R_0 \mu_0 I_p}{2\pi}$. Using a finite difference method, a spatially discretized model can be written as

$$\begin{aligned}\frac{\mathrm{d}\psi(t,x_i)}{\mathrm{dt}} = &\frac{\eta_{\parallel}(x_i)}{\mu_0 a_e^2}\left(c_1(x_i)\psi_{i+1} - c_2\psi_i + c_3(x_i)\psi_{i-1}\right) \\ &+ \eta_{\parallel}(x_i)R_0\left(j_{\mathrm{bc}}(x_i) + j_{\mathrm{nbi}}(x_i) + j_{\mathrm{eccd}}(t,x_i)\right),\end{aligned} \tag{2}$$

where $\eta_{\parallel}(x_i)$, $j_{\mathrm{bc}}(x_i)$, and $j_{\mathrm{nbi}}(x_i)$ are considered to be space-dependent parameters and $j_{\mathrm{eccd}}(t,x_i)$ is considered as a spatially distributed input. The discretization coefficients $c_1(x_i)$, c_2 and $c_3(x_i)$ agree with the chosen discretization scheme

$$c_1(x_i) = 1/2\,\frac{2x_i + \delta x}{\delta x^2 x_i}, \qquad c_2 = 2\,\frac{1}{\delta x^2}, \qquad c_3(x_i) = 1/2\,\frac{2x_i + \delta x}{\delta x^2 x_i},$$

where the index i denotes the discretization points in space, $i = 1,2,...,N$, and δx represents the characteristic length of the cell defined between two spatial discretization points [2]. The spatially discretized model (2) can now be rewritten in a state-space form, which directly suggests reachable $\psi(t,x)$ profiles, as

$$\frac{\mathrm{d}\psi_{\mathrm{i}}(\mathrm{t})}{\mathrm{dt}} = \mathbf{A}\psi_i(t) + \mathbf{B}\mathbf{u}(t) \tag{3}$$

$$y_i(t) = \mathbf{C}\psi_i(t) \tag{4}$$

where $\psi_i(t) \in \mathbb{R}^N$ is the state vector with the system matrix $\mathbf{A} \in \mathbb{R}^{N\times N}$, $\mathbf{u}(t) = \begin{bmatrix} \psi_{bc} & j_{\mathrm{ni}}(x_i) \end{bmatrix}^T \in \mathbb{R}^4$ is the input vector with the input matrix $\mathbf{B} \in \mathbb{R}^{N\times 4}$ and $y_i(t) \in \mathbb{R}^N$ is the output vector with the output matrix $\mathbf{C} \in \mathbb{R}^{N\times N}$. The state-space form of $\psi_i(t)$ is illustrated in Figure 1. The exact influence of the $j_{\mathrm{eccd}}(x_i)$ deposition, i.e. input $\mathbf{u}(t)$, on the system dynamics $\mathbf{A}$ can be quantified using the controllable subspace $\mathbb{X}^{\mathrm{con}} = \mathrm{im}\,(Co(\mathbf{A},\mathbf{B})) \subset \mathbb{R}^{\mathrm{N}}$ where Co is the controllability matrix

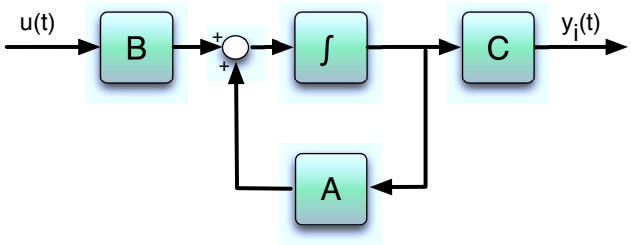

Figure 1: *Input/output block diagram.*

$$Co(\mathbf{A},\mathbf{B}) = \begin{bmatrix} \mathbf{B} & \mathbf{AB} & \mathbf{A}^2\mathbf{B} & \ldots & \mathbf{A}^{N-1}\mathbf{B} \end{bmatrix}. \tag{5}$$

The system is fully controllable if the controllability matrix has full rank, which according to the Cayley-Hamilton theorem is determined by the first $N \times N$ columns [4]. The state dimension

N represents the number of discretization points in the x-direction. For the large system with $N > 10$, there are elements of $\mathbb{X}^{\text{con}}$ that require a significant amount of energy in terms of inputs in order to be reached, and there are elements that can be easily reached [5]. The unreachable and reachable sets can be quantified using the controllability Gramian P

$$P = Co_{\infty}(\mathbf{A},\mathbf{B})Co_{\infty}^{T}(\mathbf{A},\mathbf{B}) = \sum_{i=0}^{\infty} \mathbf{A}^{i}\mathbf{B}\mathbf{B}^{T}(\mathbf{A}^{T})^{i}, \tag{6}$$

where $P \in \mathbb{R}^{N\times N}$. The elements in $\mathbb{X}^{\text{con}}$ which require the most energy to be reached have a significant component in the span of the eigenvectors of P corresponding to small absolute eigenvalues [7].

Similar to the concept of input energy, there are elements that produce more energy in terms of outputs. The observable subspaces according to the observability matrix $Ob(\mathbf{A},\mathbf{C})$ and the observability Gramian Q can be determined from the following expressions

$$Ob(\mathbf{A},\mathbf{C}) = \begin{bmatrix} \mathbf{C} \\ \mathbf{CA} \\ \mathbf{CA}^{2} \\ \vdots \\ \mathbf{CA}^{N-1} \end{bmatrix}, \qquad Q = Ob_{\infty}(\mathbf{C},\mathbf{A})Ob_{\infty}^{T}(\mathbf{C},\mathbf{A}) = \sum_{i=0}^{\infty}(\mathbf{A}^{T})^{i}\mathbf{C}^{T}\mathbf{C}\mathbf{A}^{i}.$$

The key element in determining the controllability of the $\psi_i(t)$ profile is to use the Hankel singular value decomposition (SVD) of the controllability and observability Gramians, i.e.,

$$\sigma_i = \sqrt{\lambda_i(PQ)} \quad i = 1,2,...,N. \tag{7}$$

If the SVD decrease rapidly, this means that the singular values which are approximately equal to zero $\sigma_i \approx 0$ correspond to the unreachable sets of $\psi_i(t)$. In such case, the system behavior is almost fully determined by the first few balanced states with $\sigma_i > 0$, and the minimal input/output realization is determined by the highest σ_i [6]. It is important to note that the Hankel singular value σ_i can be interpreted as the energy contribution of the i^{th} component of the balanced state to the input/output behavior of the system.

Results

Figure 2(a) illustrates the $\psi_i(t)$ time evolution of the profiles obtained by discretizing (2) with $N = 101$, whereas Figure 2(b) illustrates the first 27 largest singular values for three different stationary state regimes with constant plasma current and the space-dependent parameters obtained from CRONOS. The Hankel singular values for $\sigma_i > \sigma_{27}$ decrease rapidly. The magnetic fluxes at locations $i > 27$ that correspond to $\sigma_{28}, \sigma_{29}..., \sigma_{101}$ can only be reached with an extremely high input energy.

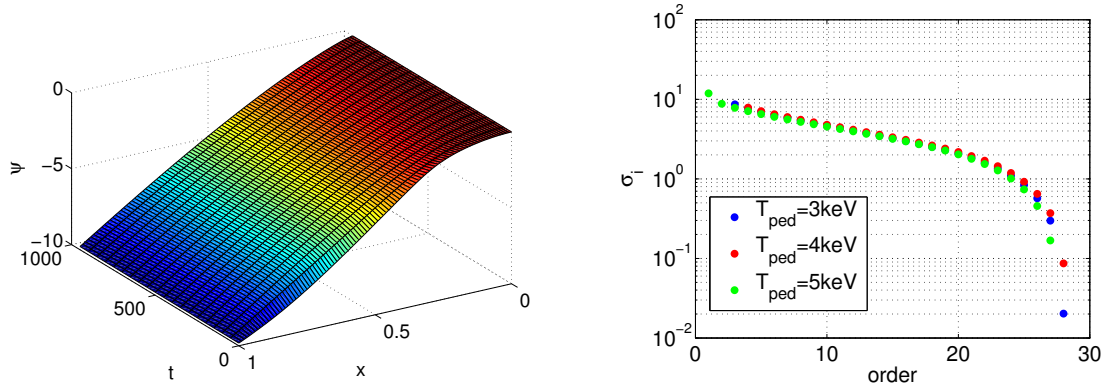

(a) (b)

Figure 2: *The system dynamics of (a) the $\psi_i(t)$ profiles in time-space and (b) the first 27 largest singular values $\sigma_1, \sigma_2 ..., \sigma_{27}$ the pedestal temperature $T_{\text{ped}} = 3\text{keV}$, $T_{\text{ped}} = 4\text{keV}$, and $T_{\text{ped}} = 5\text{keV}$, with constant plasma current $I_p = 1.2 \cdot 10^7\text{A}$.*

Discussion and conclusions

A control-oriented model has been set-up for the ITER hybrid mode. The distributed electron cyclotron current drive j_{eccd} is considered as the system input, and the distribution of the magnetic flux as the system output. A controllability analysis has been carried-out for a three realizations of the hybrid scenario in ITER with different T_{ped} profiles. The analysis indicates that the system behaves as a model of much lower order, which has to be considered for designing a real-time controller. Different actuation strategies for control designs are required in ITER both to maintain the plasma stability and to optimize the energy efficiency of the burning plasma.

Acknowledgements

This work, supported by the European Communities under the contract of Association between EURATOM/FOM, was carried out within the framework of the European Fusion Programme with financial support from NWO. The views and opinions expressed herein do not necessarily reflect those of the European Commission.

References

[1] J. Citrin *et al*, Nuclear Fusion **50** 115007 (2010)
[2] E. Witrant *et al*, Plasma Phys. Contr. Fusion **49** 1075 (2007)
[3] V. Basiuk *et al*, Nuclear Fusion **43** 822 (2003)
[4] G. Golub and C. Van Loan, Matrix computations (1996)
[5] D. Georges, Proceedings of the 34th CDC IEEE Conference, 3319 (1995)
[6] S. Shokoohi *et al*, IEEE Transactions on Automatic Control, **28** 810 (1983)
[7] B. Moore, IEEE Transactions on Automatic Control, **26** 17 (1981).